Design of light-trapping microscale-textured surfaces for efficient organic solar cells

Kanwar S. Nalwa,[1] and Sumit Chaudhary[1,2,3]*

[1]*Department of Electrical and Computer Engineering, Iowa State University, Ames, IA 50011, USA*
[2]*Department of Materials Science and Engineering, Iowa State University, Ames, IA 50011, USA*
[3]*USDOE – Ames Laboratory, Iowa State University, Ames, IA 50011, USA*
**sumitc@iastate.edu*

Abstract: Organic photovoltaic (OPV) cells suffer from low charge carrier mobilities of polymers, which renders it important to achieve complete optical absorption in active layers thinner than optical absorption length. Active layers conformally deposited on light-trapping, microscale textured, grating-type surfaces is one possible approach to achieve this objective. In this report, we analyze the design of such grating-type OPV cells using finite element method simulations. The energy dissipation of electromagnetic field in the active layer is studied as a function of active layer thickness, and pitch and height of the underlying textures. The superiority of textured geometry in terms of light trapping is clearly demonstrated by the simulation results. We observe 40% increase in photonic absorption in 150 nm thick active layer, for textures with 2 μm pitch and 1.5 μm height.

OCIS codes: (040.5350) Photovoltaic; (160.0160) Materials; (160.4890) Organic materials; (160.5140) Photoconductive materials; (250.0250) Optoelectronics; (250.2080) Polymer active devices; (050.2770) Gratings.

References and links

1. C. W. Tang, "Two-layer organic photovoltaic cell," Appl. Phys. Lett. **48**(2), 183–185 (1986).
2. P. Peumans, A. Yakimov, and S. Forrest, "Small molecular weight organic thin-film photodetectors and solar cells," J. Appl. Phys. **93**(7), 3693–3723 (2003).
3. N. S. Sariciftci, D. Braun, C. Zhang, V. I. Srdanov, A. J. Heeger, G. Stucky, and F. Wudl, "Semiconducting polymer-buckminsterfullerene heterojunctions: diodes, photodiodes, and photovoltaic cells," Appl. Phys. Lett. **62**(6), 585–587 (1993).
4. G. Yu, and A. J. Heeger, "Charge separation and photovoltaic conversion in polymer composites with internal donor/acceptor heterojunctions," J. Appl. Phys. **78**(7), 4510–4515 (1995).
5. J. J. M. Halls, C. A. Walsh, N. C. Greenham, E. A. Marseglia, R. H. Friend, S. C. Moratti, and A. B. Holmes, "Efficient photodiodes from interpenetrating polymer networks," Nature **376**(6540), 498–500 (1995).
6. G. Yu, J. Gao, J. C. Hummelen, F. Wudl, and A. J. Heeger, "Polymer photovoltaic cells: enhanced efficiencies via a network of internal donor-acceptor heterojunctions," Science **270**(5243), 1789–1791 (1995).
7. W. L. Ma, C. Y. Yang, X. Gong, K. Lee, and A. J. Heeger, "Thermally stable, efficient polymer solar cells with nanoscale control of the interpenetrating network morphology," Adv. Funct. Mater. **15**(10), 1617–1622 (2005).
8. G. Li, V. Shrotriya, J. Huang, Y. Yao, T. Moriarty, K. Emery, and Y. Yang, "High-efficiency solution processable polymer photovoltaic cells by self-organization of polymer blends," Nat. Mater. **4**(11), 864–868 (2005).
9. R. J. Kline, M. D. McGehee, E. N. Kadnikova, J. Liu, and J. M. J. Fréchet, "Controlling the field-effect mobility of regioregular polythiophene by changing the molecular weight," Adv. Mater. **15**(18), 1519–1522 (2003).
10. M. Agrawal, and P. Peumans, "Broadband optical absorption enhancement through coherent light trapping in thin-film photovoltaic cells," Opt. Express **16**(8), 5385–5396 (2008).
11. P. Campbell, and M. A. Green, "Light trapping properties of pyramidally textured surfaces," J. Appl. Phys. **62**(1), 243–249 (1987).
12. C. Heine, and R. H. Morf, "Submicrometer gratings for solar energy applications," Appl. Opt. **34**(14), 2476–2482 (1995).
13. L. Stolz Roman, O. Inganäs, T. Granlund, T. Nyberg, M. Svensson, M. R. Andersson, and J. C. Hummelen, "Trapping light in polymer photodiodes with soft embossed gratings," Adv. Mater. **12**(3), 189–195 (2000).

#121420 - $15.00 USD Received 14 Dec 2009; revised 17 Feb 2010; accepted 17 Feb 2010; published 25 Feb 2010

14. M. Niggemann, M. Glatthaar, A. Gombert, A. Hinsch, and V. Wittwer, "Diffraction gratings and buried nano-electrodes - architectures for organic solar cells," Thin Solid Films **451–452**, 619–623 (2004).
15. L. A. A. Pettersson, L. S. Roman, and O. Inganäs, "Modeling photocurrent action spectra of photovoltaic devices based on organic thin films," J. Appl. Phys. **86**(1), 487–496 (1999).
16. F. C. Chen, J. L. Wu, C. L. Lee, W. C. Huang, H. M. P. Chen, and W. C. Chen, "Flexible Polymer Photovoltaic Devices Prepared With Inverted Structures on Metal Foils," IEEE Electron Device Lett. **30**(7), 727–729 (2009).
17. M. Glatthaar, M. Niggemann, B. Zimmermann, P. Lewer, M. Riede, A. Hinsch, and J. Luther, "Organic solar cells using inverted layer sequence," Thin Solid Films **491**(1-2), 298–300 (2005).
18. E. Lioudakis, A. Othonos, I. Alexandrou, and Y. Hayashi, "Optical properties of conjugated poly(3-hexylthiophene)/[6,6]-phenylC_{61}-butyric acid methyl ester composites," J. Appl. Phys. **102**(8), 083104 (2007).
19. L. A. A. Pettersson, F. Carlsson, O. Inganäs, and H. Arwin, "Spectroscopic ellipsometry studies of the optical properties of doped poly(3,4-ethylenedioxythiophene): an anisotropic metal," Thin Solid Films **313–314**(1-2), 356–361 (1998).
20. J. Bartella, J. Schroeder, and K. Witting, "Characterization of ITO- and TiO_xN_y films by spectroscopic ellipsometry, spectraphotometry and XPS," Appl. Surf. Sci. **179**(1-4), 181–190 (2001).
21. P. B. Johnson, and R. W. Christy, "Optical constants of transition metals: Ti, V, Cr, Mn, Fe, Co, Ni, and Pd," Phys. Rev. B **9**(12), 5056–5070 (1974).
22. D. W. Sievers, V. Shrotriya, and Y. Yang, "Modeling optical effects and thickness dependent current in polymer bulk-heterojunction solar cells," J. Appl. Phys. **100**(11), 114509 (2006).

1. Introduction

Polymer and small-molecule based OPVs have gained a lot of attention in the last decade due to their potential low cost and roll-to-roll manufacturing capability, and amenability to flexible substrates. Most of the developments that have improved performance of OPVs are based on electron donor-acceptor (D-A) heterojunctions. In a planar heterojunction, or 'bilayer' device, excitons are dissociated into charge-carriers at the D-A interface. The efficiency of PV conversion is however low because only the excitons created within the exciton-diffusion length from the D-A interface are utilized [1–3]. A revolutionary development in OPVs came in the mid-1990s with the introduction of bulk-heterojunction OPVs, in which the D-A materials are blended together [4–6]. If the length scale of the phase-separation in D-A blend is similar to the exciton-diffusion length, then all excitons photogenerated in either material are likely to diffuse to an interface and dissociate into free charge carriers. These charge carriers are then drifted to the respective electrodes if continuous pathways exist in each material. The electron acceptors are often the fullerenes or their derivative [6,6]-phenyl-C61-butyric acid methyl ester (PCBM) having better miscibility in organic solvents. For OPVs with poly(3-hexylthiophene) as electron donor, highest efficiencies reaching up to 5% have been reported [7,8].

The performance of these bulk heterojunction devices is still limited by several factors. The high energy band gap of the most polymer materials poses a serious limitation on the capability to harvest lower energy photons from sunlight. Moreover, the charge carrier mobility of these materials is low [9], making it necessary to keep the thickness of the active layer low. A thinner film between the electrodes can lower the probability for charge recombination, and increase the carrier drift velocity due to higher electric field. However, the optical absorption will be low in such thin films. Thus, there is a conflict between the optical and the electronic length-scales. A unified concept of anti-reflection coatings and distributed Bragg reflectors is one method recently suggested to increase the absorption in thin OPV films [10]. Another way to resolve this conflict can be a textured, grating-shaped OPV cell geometry. Submicron or micron structures can modify the incident wave momentum in such a way that the incident light remains trapped in the solar cell active layer due to total internal reflection at the interfaces [11,12]. This results in increased absorption in the active layer, and facilitates the use of layers with optimum thickness with regard to the electrical properties. The perceived optoelectronic benefits of using these light trapping structures have led to the recent development of embossing being successfully applied to the patterning of polymer OPVs, leading to a significant increase in generated photocurrent [13]. A more recent work focused on enhancing absorption in the active layer by implementing light trapping structures like diffraction-gratings and buried nano-electrodes [14]. However, in these reports, study was

#121420 - $15.00 USD Received 14 Dec 2009; revised 17 Feb 2010; accepted 17 Feb 2010; published 25 Feb 2010

carried out for a single pitch and active layer thickness. What should be the optimum dimensions of a micron or submicron-scale grating in OPVs – is an open question. In the present study, we therefore investigate in detail, the effect of pitch, height and active layer thickness on the performance of grating-based textured OPVs. It should be noted that similar studies for silicon-based solar cells [11,12] are not directly relevant for OPVs due to difference in active layer thicknesses between these two technologies. For thin-film silicon solar cells, grating structures serve more of a back reflector role for a thicker active layer. However, in OPVs, active layer will be much thinner and conformal with the textured surfaces.

For planar solar cells, optimization has been performed using optical models based on transfer matrix formalism for normal light incidence [15]. This approach however is not suitable for the optical modeling of textured grating-based OPV cells, since the grating pitch is of the order of wavelength of light leading to complex diffraction and interference effects that have to be included in the model. Finite element model inbuilt in COMSOL MULTIPHYSICS has been used to perform the simulations, accounting for the three-dimensional geometry and wavelength dependence of dielectric functions for materials. Optical modeling was performed to calculate an optimum grating geometry and to gain a better understanding of the light absorption in the textured solar cells. The energy dissipation of electromagnetic field in the active layer was studied as a function of active layer thickness, grating pitch and height.

The evaluated cells consist of four layers: ITO (100nm), poly(3,4 ethylene dioxythiophene):poly(styrene sulfonate) (PEDOT:PSS)~50nm, P3HT:PCBM blend(1:1) as the active layer and titanium (250nm). The active layer thickness was varied keeping the thickness of other layers constant. The cells have inverted geometry, with ITO on the top and Ti as bottom electrode, allowing light incidence from the top. In practice, ITO layer can be sputtered on the top of a protective buffer layer such as MoO_3 to prevent degradation of PEDOT layer from plasma exposure [16]. ITO is required for top illumination and direct comparison of textured OPVs with bottom illuminated planar cells on ITO substrate. Ti is used instead of Al as bottom electrode since oxidation of Al leads to degradation of electrical contact and inverted solar cell structures employing Ti as bottom contact have been demonstrated earlier [17].

2. Simulation setup

The simulations were performed on the tapered structures depicted in Fig. 1, with a series of stacked layers with different optical properties. For use in our model, the complex refractive indices ($n + ik$) as a function of wavelength were obtained from the literature [18–21]. In the simulations, light enters from air, and is incident on the OPV cell at air-ITO interface. In the case of textured solar cells, the incident wave was generated at a boundary, with a condition allowing the generated wave to enter the structure, and the wave reflected from the structure to be transmitted through this boundary, into a perfectly matched layer. This perfectly matched layer is simulating the semi-infinite surrounding by absorbing all the outgoing waves

#121420 - $15.00 USD Received 14 Dec 2009; revised 17 Feb 2010; accepted 17 Feb 2010; published 25 Feb 2010

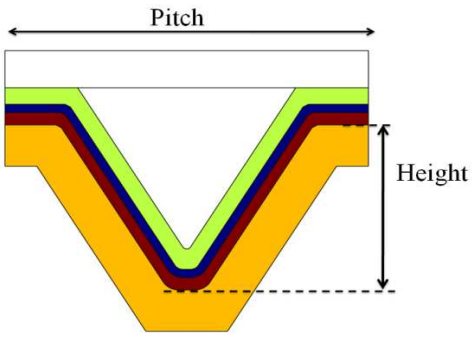

Fig. 1. Structure of the modeled grating-based OPV cell. At the bottom is a Ti layer, on which the P3HT:PCBM active layer, the PEDOT:PSS layer, and the ITO layer are sequentially located.

with a minimum of reflections. In order to avoid complexity, the anisotropy of dielectric function found in some materials is not represented in this model. The electromagnetic wave equations were solved on the entire defined geometry taking into account the interference, refraction and reflection effects. In order to fix the geometry of the textured devices used for simulations, irrespective of the pitch, slope of the grating was kept constant for structures having same aspect ratio (pitch:height). Moreover, opening (7/10th of pitch) and bottom width (1/10th of pitch) of the grating was kept same for a given pitch size and varied proportional to the pitch size. The range of wavelengths chosen for the simulations is 300-700 nm with incident power being defined by AM 1.5 sun light spectra. Since different pitch structures had different area sizes exposed to the incoming solar flux, the incident power was normalized with respect to 1μm pitch size, giving it the unit of W/m^2. The electromagnetic power dissipation per volume, Q, in the active layer is studied as a criterion to optimize the height and pitch of the structures as well as the active layer. The total power absorbed (W/m^2) in a layer was calculated by integrating Q over the active layer space, summing over all the wavelengths and then normalizing with respect to the 1 μm pitch.

3. Experimental details

The modeled data for the planar configuration was compared with experimental results to verify the accuracy of refractive indices used in the simulations. Planar structures were fabricated with similar layer sequence as their modeled counterparts. A titanium layer was evaporated on cleaned glass slide. The P3HT:PCBM blend with 1:1 weight ratio was used. P3HT concentration was 17 mg/ml in dichlorobenzene solution. The blend solution was spin coated on top of the titanium layer. A conducting film of PEDOT:PSS was spin coated on the photoactive layer to act as anode. Reflectance of this structure was measured using Varian Cary 5000 UV-Vis-NIR spectrophotometer and used as a criteria for authenticity of optical constants employed in simulations.

4. Results and discussion

In order to confirm and validate the simulation results of FEM model, simulations of planar stacked layers were performed with the use of transfer matrix method (TMM) and compared with the FEM results on the same. The results of FEM and TMM simulations on planar OPV cell showed good agreement. Simulations on fabricated planar structure were performed with the layer thicknesses obtained from surface profiler measurements to predict the reflectance. A good fit between the measured and simulated reflectance is obtained as shown in Fig. 2. A small deviation is exhibited which can be due to non homogenous spin coated layers.

Figure 3 shows the variation of energy dissipation in the active layer with for different pitches and heights of the grating structure. The results reveal that absorption is least for 500 nm pitch, which can be attributed to the increased reflection of higher order diffracted light

#121420 - $15.00 USD Received 14 Dec 2009; revised 17 Feb 2010; accepted 17 Feb 2010; published 25 Feb 2010

when grating period is less than the wavelength of light. With 1μm pitch, the grating period is more than the relevant wavelengths, hence reflection of light due to higher order diffraction will be low, leading to light trapping effects in the active layer. It is also observed that 1 μm pitch structure with 750 nm height (aspect ratio 4:3) leads to highest absorption in the active layer. For 2 μm pitch also, the same aspect ratio (4:3) leads to highest absorption. As the height of the structure increases, the effective volume of active layer available for absorption increases too. However, the grating becomes narrower and the coupling of light decreases. These two trends have a push and pull effect on the optimum height for highest absorption.

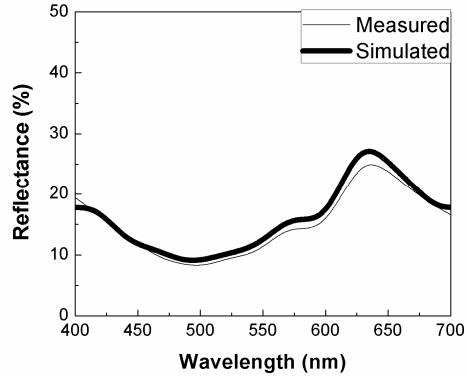

Fig. 2. Measured and simulated reflectance from planar cell. Layer thicknesses used in the simulations are PEDOT:PSS: 50 nm and active layer: 70 nm.

For pitch size of 4 μm, bulk effects start dominating and diffraction effects become small. Hence, the only parameter that affects the absorption in 4 μm pitch structures is the volume of the active layer which increases with the height of grating. Overall, the structure with 2μm pitch and 1.5 μm height showed highest absorption of incident power in the active layer and hence appears to be most promising among all the micro-regime dimensions. This structure is accompanied with 36% increment in energy dissipation inside the 75 nm thick active layer with respect to the planar cell. The energy dissipation relative to corresponding planar cell is greater than unity for all the textured geometries irrespective of their pitch and height, which can be explained by contributions from increased light concentration and effective area.

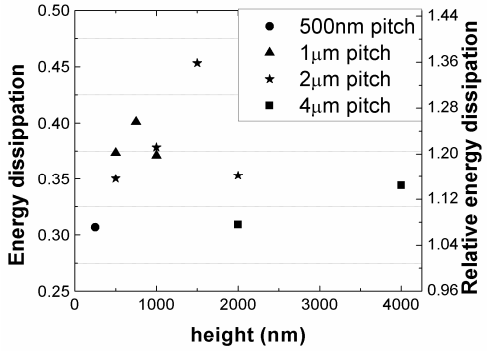

Fig. 3. (left) Energy dissipation (as fraction of incident power) in the active layer, as a function of height and pitch of the grating. Active layer thickness is 75 nm. Thickness of PEDOT:PSS and ITO is 50 and 100 nm, respectively. Right hand side axis has energy dissipation in active layer relative to corresponding planar cell.

The energy dissipation inside textured devices at 500 nm wavelength [important for photocurrent generation in P3HT-based OPVs) for 2 μm pitch - 1.5 μm height, and 1 μm pitch - 750 nm height structures is plotted in Fig. 4(a) and 4(b). The excitation beam is transverse

#121420 - $15.00 USD Received 14 Dec 2009; revised 17 Feb 2010; accepted 17 Feb 2010; published 25 Feb 2010

electric (TE) polarized, i.e., with a polarization along the grating stripes. The bright spots in the active layer show the maximum energy dissipation regions. In case of TE polarized light, power flow gets channeled in these regions as shown by arrows and results in the focusing of electromagnetic energy inside the active layer (Fig. 4(a) and 4(b)]. This feature originates directly from the diffraction of a part of the incident light on to tapered structure, according to the following formula:

$$k_d \sin\theta_d = \pm ki \sin\theta_i \pm \frac{2\pi m}{\Lambda} \quad (1)$$

where Λ is the width of the tapered structure at some height, k_i (k_d) is the incident (diffracted) light wave vector, θ_i (θ_d) is the light incident (diffracted) angle, and m is an integer corresponding to the diffraction order.

The region where the incident light is diffracted with an angle θ_d, greater than the angle that slope of grating makes with normal i.e. θ_c as shown in Fig. 4(a), standing wave will be formed. This wave is confined by total internal reflection at the polymer/air interface and the metal grating reflection. A part of the light will then propagate and get dissipated in the active layer, leading to an enhancement in the absorption around that region. In the present case of normal incidence ($\sin\theta_i = 0$), Eq. (1) can be simplified to following form:

$$\sin\theta_d = \pm \frac{m\lambda}{\Lambda n} \quad (2)$$

where λ is the wavelength of light and n is the refractive index. From Eq. (2) it can be deduced that the diffraction angle will be small where width is large and hence the diffracted light will escape the structure without getting coupled into the polymer layer. For effective coupling to take place, the diffracted light has to be guided parallel to the slope of the tapered structure which happens when width becomes sufficiently small. This is the reason why maximum energy dissipation takes place approximately at the same opening width for the two structures of Fig. 4(a) and 4(b), having same aspect ratio or slope (4:3) at 500nm wavelength. Similar results were obtained for other aspect ratios dealt in this study (not shown here). Figure 4(c) clearly evidences that in case of TM polarized light, the power flow is along the incident wave propagation direction and almost unaffected by the grating. This is similar to the case of planar cell (Fig, 4(d)) and therefore doesn't lead to significant enhancement in absorption.

From Fig. 5(a), the ratio of maximum absorption height level and the total height of grating is found to decrease on increasing the pitch. This is because the width at which light diffraction suitable for trapping takes place, lies closer to the bottom of the grating for bigger pitches. On decreasing the aspect ratio, the grating structure becomes narrower and hence the energy concentration region shifts farther from the bottom of the grating. This explains the reason for lower aspect ratio having larger ratio of maximum absorption height and height of grating for a fixed pitch, as shown in Fig. 5(a). For 2µm pitch-1.5µm height grating structure, the maximum absorption height increases with increasing wavelength of incident TE polarized light as seen in Fig. 5(b). This result can be explained by using Eq. (2), according to which, wavelength of the light diffracted parallel to the slope of grating i.e. $\theta_d = \theta_c$, is proportional to the grating's width for standing wave formation.

#121420 - $15.00 USD Received 14 Dec 2009; revised 17 Feb 2010; accepted 17 Feb 2010; published 25 Feb 2010

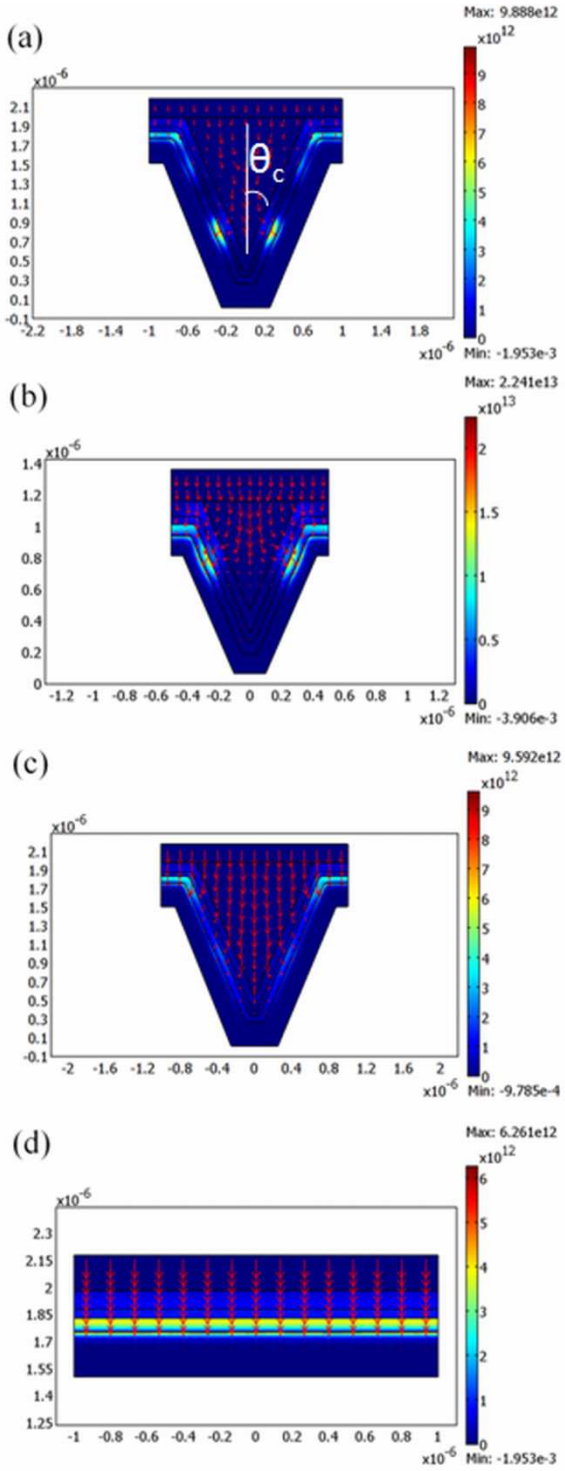

Fig. 4. Energy dissipation (W/m^3) colored map at 500 nm wavelength of light for (a) TE polarization in 2 μm pitch - 1.5 μm height (b)TE polarization in 1 μm pitch – 750nm height and (c) TM polarization in 2 μm pitch - 1.5 μm height (d) Flat structure, with arrows showing power flow (time averaged). The thicknesses of ITO, PEDOT:PSS and active layer are 100, 50 and 75 nm respectively. Unit is meters for geometry.

#121420 - $15.00 USD Received 14 Dec 2009; revised 17 Feb 2010; accepted 17 Feb 2010; published 25 Feb 2010

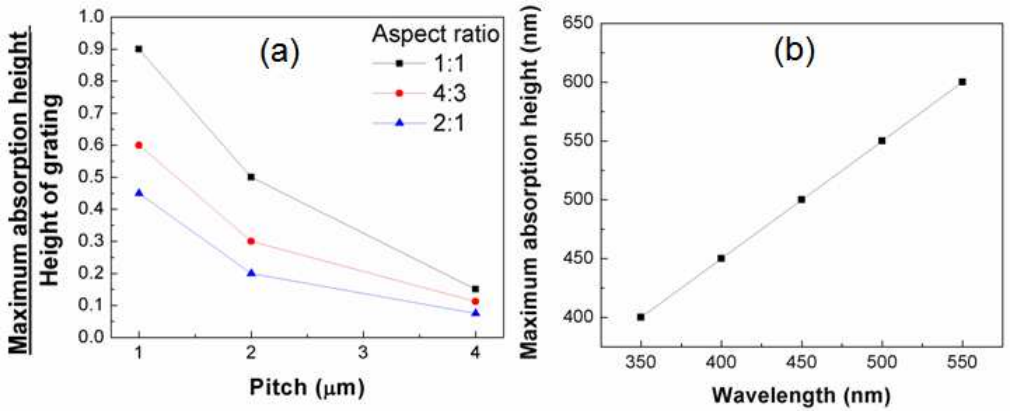

Fig. 5. (a) Dependence of the ratio of maximum absorption height and height of grating on pitch size for 1:1, 4:3 and 2:1 aspect ratios for TE polarized light of 500nm wavelength. (b)Variation of maximum absorption height with wavelength of TE polarized excitation light in 2μm pitch-1.5μm height grating structure. The thicknesses of ITO, PEDOT:PSS and active layer are 100, 50 and 75 nm respectively.

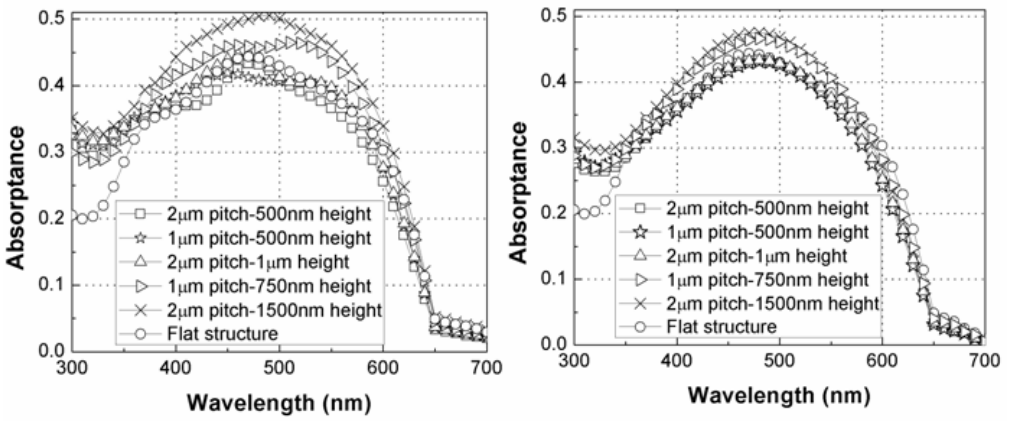

Fig. 6. Absorptance in 75 nm thick active layer for various textured structures and flat cell with PEDOT:PSS and ITO layer thickness of 50 and 100 nm, respectively in the case of TE (left) and TM (right) polarizations of incident light.

Higher photonic absorption in the textured structures arises mostly from the guiding of diffracted TE polarized part of incident light in the polymer layer with little enhancement from TM polarization, as seen in Fig. 6. In the case of TM polarized excitation beam, a small increment in the absorption for all grating structures relative to the planar cell can be a consequence of increased area available for absorption in grating structures. The dip in the absorption below 350 nm in the planar cell is accordingly filled up and almost removed by making use of textured structures, as displayed in Fig. 6. The thickness of the active layer studied (75 nm) is less than the absorption length at short wavelengths too. Therefore, some of the absorption enhancement for short wavelength (300-500nm) comes from coupling of incident light into the modes that are guided in the active layer, hence enhancing the light travelling path and providing a light trapping mechanism. Remaining enhancement can be attributed to better effective refractive index matching with air (antireflection effect) that suppresses light reflection significantly. The wave guiding effect is particularly important for long wavelength regime where the active layer is less absorptive and a single path cannot absorb all the incident light. This can be elucidated by appreciable absorptance enhancement ratio at wavelengths longer than 550 nm, as shown in Fig. 7.

#121420 - $15.00 USD Received 14 Dec 2009; revised 17 Feb 2010; accepted 17 Feb 2010; published 25 Feb 2010

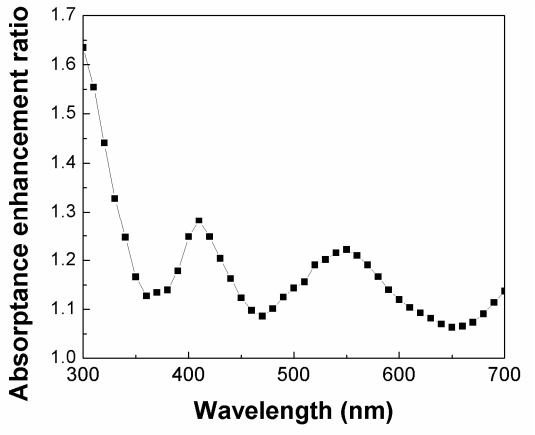

Fig. 7. Absorptance enhancement ratio (Absorptance ratio of 2 μm pitch-1.5 μm height grating and flat cell) as a function of wavelength for 75 nm thick active layer. The thicknesses of PEDOT:PSS and ITO layers are 50 and 100 nm respectively.

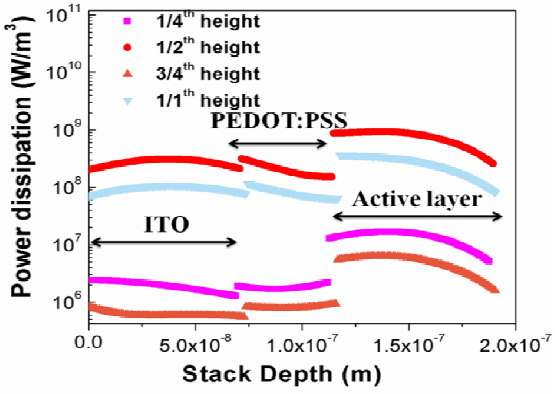

Fig. 8. Energy dissipation at 1/4, 1/2, 3/4 and 1 of the height, measured from the bottom of the 2 μm pitch - 1.5 μm height grating. Thicknesses of ITO, PEDOT:PSS and active layer are 75, 40 and 75 nm respectively.

Figure 8 shows energy dissipation profiles perpendicular to the layers and at different heights from the bottom of our most promising 2 μm pitch - 1.5 μm height textured cell. The intensified energy dissipation caused by the confinement of electromagnetic wave in the structure can be seen, with largest absorption occurring at 1/2 height. This light trapping is also evident from Fig. 9 which shows the effect of active layer thickness on the absorption for textured (2 μm pitch - 1.5 μm height) and planar OPVs with 100 nm, and 50 nm thick ITO and PEDOT:PSS layers, respectively. Although the absorption increases with the increasing thickness of the active layer for both geometries - planar as well as textured - it is observed that the absorption relative to the corresponding planar cell is maximum for 150 nm thick active layer (1.5 and 1.3 times for TE and TM modes, respectively) as displayed in the insets of Fig. 9. The observation that absorption enhancement as a result of texturing has a maxima and is not a monotonically decreasing function of active layer thickness is attributed to interference effects, making some layer thicknesses more beneficial for energy trapping. The absorption at higher active layer thicknesses (200-250nm) saturates, indicating that there is very little light that is reflected or absorbed in the metal and is left to be absorbed in the photoactive layer. This has an important implication for textured geometries - that the 150 nm active layer thickness is not only competitive with the 250 nm thickness in terms of absorption, but it will also significantly improve the carrier transport [22].

#121420 - $15.00 USD Received 14 Dec 2009; revised 17 Feb 2010; accepted 17 Feb 2010; published 25 Feb 2010

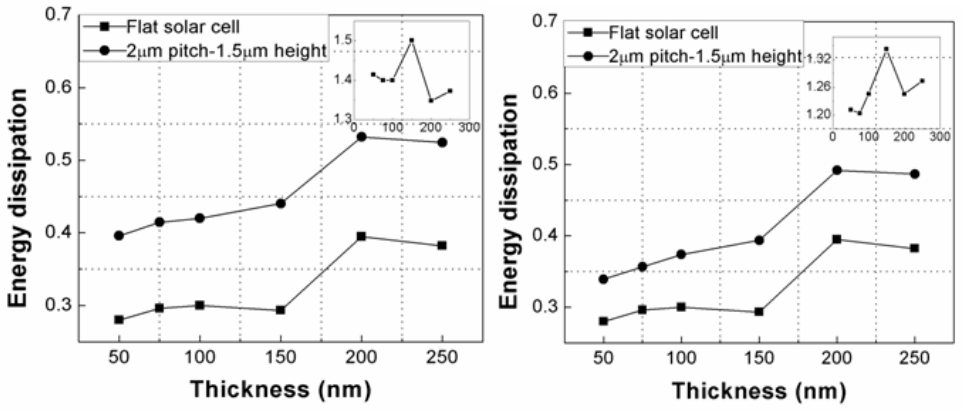

Fig. 9. Variation of energy dissipation (as fraction of incident power) in the active layer for different active layer thickness for textured (2 μm pitch - 1.5 μm height) and planar OPV cell in case of TE (left) and TM (right) polarizations of incident light. Inset graph in the top right corner displays energy absorbed in textured relative to planar cell as a function of active layer thickness.

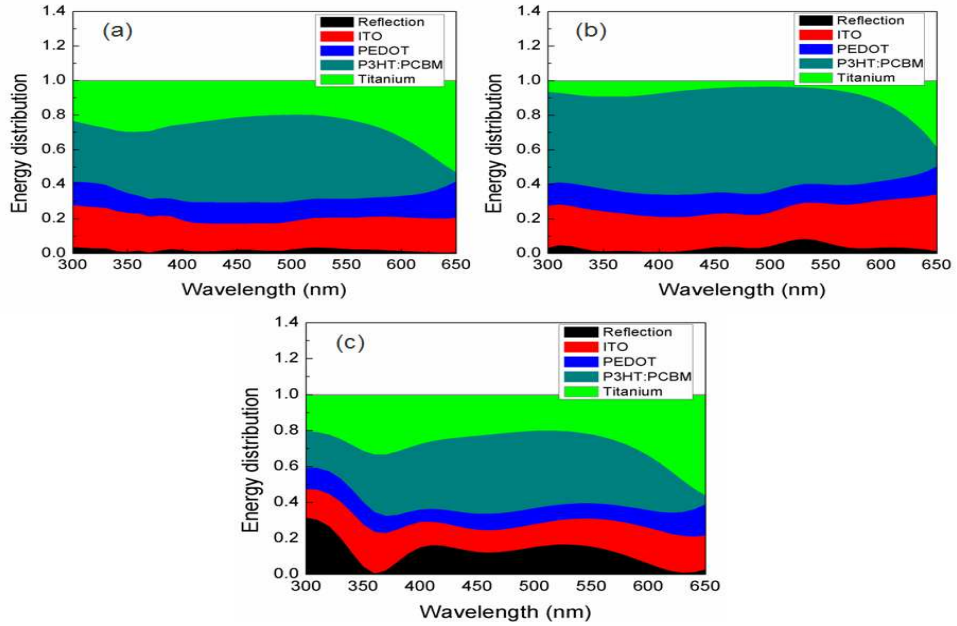

Fig. 10. Energy dissipation maps in (a) 2 μm pitch-1.5 μm height grating with 75 nm thick active layer (b) 2 μm pitch-1.5 μm height grating with 250 nm active layer thickness (c) flat cell with 75nm active layer thickness. Thickness of PEDOT:PSS and ITO is 50 and 100 nm respectively.

Energy dissipation maps are plotted for 2 μm pitch-1.5 μm height grating with 75 and 250 nm thick active layer [Fig. 10(a) and (b)] and compared with a flat cell with 75nm active layer thickness [Fig. 10(c)]. For the same thickness of active layer, textured cell shows a significantly smaller reflectance than planar cell, due to the increased absorption in the active layer as well as in ITO. On increasing the thickness of active layer from 75nm to 250nm for the 2 μm pitch-1.5 μm height structure, the enhanced absorption in the polymer layer is mostly induced by reduction of energy dissipation inside the metal.

#121420 - $15.00 USD Received 14 Dec 2009; revised 17 Feb 2010; accepted 17 Feb 2010; published 25 Feb 2010

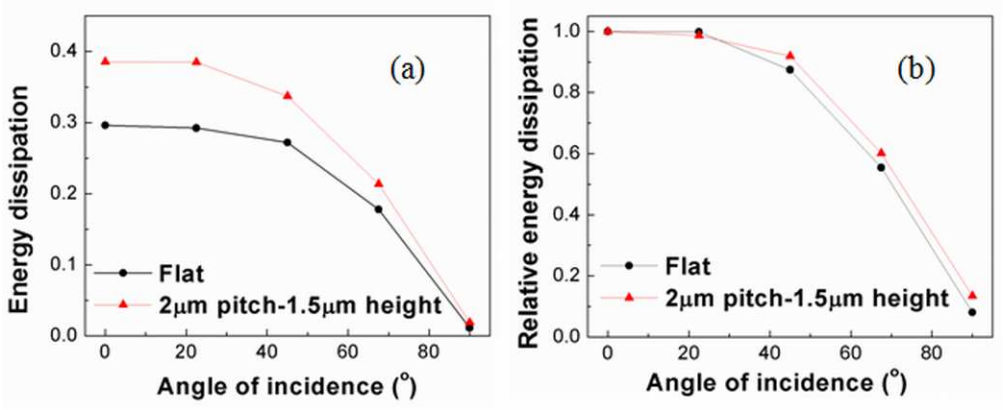

Fig. 11. (a) Energy dissipation (as a fraction of incident power) and (b) Relative Energy dissipation (as fraction of energy dissipated at 0° or normal incidence) (right) in 75 nm thick active layer (P3HT /PCBM) as a function of incident angle, for flat and 2 μm pitch-1.5 μm height grating. Layer thicknesses used in the simulations are PEDOT:PSS: 50nm and ITO: 100nm.

For solar cells in a practical environment where sunlight can be quite diffused, it is important to evaluate the absorptance over a wide range of incident angles. Figure 11(a) suggests that 2 μm pitch-1.5 μm height grating structure has a distinguished advantage over flat device for all incident angles and thus in the real environment. The absorption efficiency of flat surface drops more abruptly as the incident angle increases when compared to grating structure, as shown in Fig. 11(b). Higher relative energy dissipation [Fig. 11(b)] in grating structure is attributable to the suppression of reflection loss.

5. Conclusions

Using the finite element method, we have modeled the optical behavior of microscale textured OPVs in comparison with the conventional planar geometry. A maximum of 40% increase in photonic absorption is observed in active layer (150nm) for grating-type bottom electrode with 2 μm pitch and 1.5 μm height texture. Our results show that if an OPV active layer is conformally deposited on a textured electrode, it is possible to achieve optimal photonic absorption in thinner active layers, which will lead to improved charge transport and higher efficiencies in OPVs. The proposed approach, thus, offers a potential solution towards the classic conflict between optical and electronic scales in OPVs. We do realize that it will not be straightforward to conformally deposit active layers on proposed textured surfaces, if processed from solution using techniques like spin-coating, which are more amenable to flat surfaces. Some tailoring and innovation would thus be required on the processing front for polymer based OPVs. However, our results are immediately applicable to small-molecule based OPVs that utilize thermal-evaporation for deposition for active layers. In addition, our approach can also have potential implications on the fields of photodetectors, photoelectrochemical systems, and the like.

Acknowledgements

We thank Iowa State University for start-up funds, Iowa Power Fund from the state of Iowa's Office of Energy Independence, and USDOE Ames Laboratory for seed funding. We also thank Dr. Jayeoun Kim and Dr. Kai-Ming Ho for helpful discussions.

#121420 - $15.00 USD Received 14 Dec 2009; revised 17 Feb 2010; accepted 17 Feb 2010; published 25 Feb 2010